

Calibration and 3D Ground Truth Data Generation with Orthogonal Camera-setup and Refraction Compensation for Aquaria in Real-time

Klaus Müller, Jens Schlemper, Lars Kuhnert and Klaus-Dieter Kuhnert

Institute of Realtime Learning Systems, Department of Electrical Engineering and Computer Science, University of Siegen, Hölderlinstr. 3, 57076 Siegen, Germany

Keywords: Calibration, Fish Tank, Refraction, 3D-model, Tracking, Vision, Segmentation.

Abstract: In this paper we present a novel approach to generate precise 3D ground-truth data considering the refraction of the fish tank. We used an accurate and easy-to-handle calibration method to calibrate two orthogonally aligned high-resolution cameras in real-time. For precise fish shape segmentation we combined two different background subtraction algorithms, which can also be trained while fish are swimming inside the aquarium. The presented approach takes also shadow segmentation removal and mirroring into account. For refraction compensation at the air-water border we developed an algorithm which calculates the ray-deflection of every shape-pixel and compute the 3D-model in real-time.

1 INTRODUCTION

In fish behaviour studies computer vision is a well known tool to observe fish's position and movements. One of the main research areas in this scope is the study of mate-choice. The classical approach for mate choice studies is laborious and time-consuming, due to the fact, that real mate's behaviour is undefined and hardly repeatable.

The presented work is part of an interdisciplinary project between computer science and biology. The aim of the project is to create a virtual fish which interacts with real fish for conducting strictly-controlled behavioural mate-choice-studies. At first fish's movements and behaviour have to be analysed with the help of a computer vision system. In the sequel the gathered information is used to create a photo-realistic simulation of fish and their behaviour. The used fish species is *sailfin molly* (see Figure 1), which has a size of 4 to 10 cm and is able to move quite quickly and rather abruptly. Especially, its quick movements place special demands on the computer vision system.

In a future step, a fish model will be created with



Figure 1: Sailfin mollies.

the help of the gathered shape, movement and behaviour information of the species. This steerable virtual fish may be used by the behaviour scientists to conduct fish-behaviour experiments under strictly controlled conditions. With the help of the tracking information of the real fish the virtual fish projected onto a screen can react to and also interact with the real fish. Furthermore the model will be utilised to build a tracking system based on a model-based approach using an appearance model of the fish (analysis-by-synthesis). The analysis-by-synthesis method allows to track the fish's 3D-position and 3D-deformation by using only one camera. Due to the model's information about the fish's movements the algorithm renders the most probable image of the virtual fish and compares this to the captured image of the real fish. This step is repeated until the rendered image becomes undistinguishable from the captured image. As a result the algorithm provides the best fit model parameters and consequently a complete fish description in 3D.

In this paper we describe the first period of this project. Besides the setup of the computer vision system, we also developed a segmentation and reconstruction system to get precise ground truth data of the fish's position, pose and movement under consideration of refraction at the air-water-boarder. On the one hand this is the precondition for creating a virtual fish, on the other hand this allows to quantitatively evaluate the results stemming from the new analysis-

by-synthesis approach later on.

The future system will be able to handle multiple fish. Due to the fact that the main focus of this paper lies on calibration, segmentation and refraction-compensation, we conduct our tests with a single fish and do not take occlusion (fish-fish) into account.

2 BACKGROUND AND METHODS

For the following experiments we use a fish tank with the size of 600 mm x 300 mm x 300 mm.

2.1 Computer Vision Setup

Due to the fact that computer vision systems became more powerful and easier to use their number in animal behaviour studies has increased during the last years (Delcourt et al., 2012). Especially in fish-behaviour projects it is a very important tool to observe fish's movement, position and consequently its behaviour. During the last years besides two-dimensional tracking systems (e.g. (Fontaine et al., 2008)) also three-dimensional tracking systems have been established ((Zhu and Weng, 2007); (Butail and Paley, 2012)). For the latter one different types of vision systems are used in fish behaviour studies.

2.1.1 Camera Setup and Illumination

The method described in Laurel et al. (Laurel et al., 2005) is based on fish shadows. They installed two lamps above the aquarium and recorded the fish and their shadows with one camera. With the help of trigonometric computations they calculated the fish's positions. For increasing numbers of fish this kind of tracking system is not suitable caused by the occlusions of multiple shadows. Zhu and Weng (Zhu and Weng, 2007) extended their fish tank with mirrors above and on the left side of the aquarium. Besides the front view the camera placed in front of the aquarium also recorded the mirrored top and left view. By doing so this system is also suitable for bigger fish groups. Butail and Paley (Butail and Paley, 2012) used three orthogonal cameras, placed above, in front and on the left side of the fish tank. They reconstructed fish bodies by extracting ellipses from fish images of two cameras and combining them to an ellipsoid in a post processing step. The left camera was used for validation of the tracking result.

For our future analysis-by-synthesis tracking-approach we need high resolution coloured pictures of the fish. Additionally initial tests showed that the

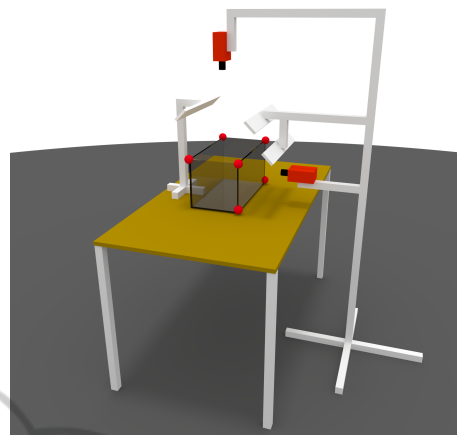


Figure 2: Camera system with illumination. The fish tank is equipped with red marker balls.

fish can turn their body within 100 ms around 180° what places special demands on the camera. For that reasons we chose two gigabit ethernet color cameras (Allied Vision Technologies, Prosilia GT1910c) with a resolution of 1920 x 1080 and with a frame rate of 57 frames per second. The cameras were synchronised by a hardware trigger and connected over gigabit ethernet to a stationary PC (quad core CPU Intel i5-2320 3 Ghz, two Gigabit Ethernet cards, RAID0 system). The cameras produce 220 MB of raw data per second. For 3D calculation we chose a camera setup similar to (Butail and Paley, 2012). We mounted the cameras on a fixed frame. The first one was placed above and the second one in front of the fish tank. For illumination we chose LED stripes placed on both sides at an angle of 45° above the tank (see Figure 2). In contrast to other systems in this scope (Fontaine et al., 2008; Butail and Paley, 2012; Yamashita et al., 2011) our system is real-time capable.

2.1.2 System Infrastructure

Given that the final system will be used for interactive fish behaviour studies in future it will consist of several subsystems placed on different computers. Based on this assumption every part of the system (tracking system, observer control system and 3D-fish engine) has to communicate with each other in real time. Owing to this fact a suitable communication system is necessary. Due to our former positive experience with the robot operating system ROS (Quigley et al., 2009) in context of distributed systems and multi sensor networks (Kuhnert et al., 2012) we decided to use this system in this project, too. Besides, the easy communication over Ethernet between all sensors and software modules, ROS includes a huge toolbox for

recording and manipulating sensor data.

2.2 Camera Calibration

For three-dimensional object-tracking with two cameras accurate camera calibration is very essential. Especially in field of fish-tracking in aquariums refraction places special demands on the calibration method. Butail and Paley (Butail and Paley, 2012) used in their paper the camera calibration toolbox of Matlab (Bouguet, 2004). For calibration they filmed a planar checkerboard underwater at different orientations. Their method does not take the air-water refraction into account and they assumed that this caused inaccuracies. Yamashita et al. (Yamashita et al., 2011) used omni-directional stereo cameras for underwater sensing. These were placed above each other in an acrylic cylindrical waterproof case. For refraction compensation Yamashita et al. used an optical ray tracing technique. For our purpose it is very important that the calibration system is easy and fast to handle hence the experiment conductors can calibrate it themselves after an accidental camera displacement during the experiments. For the intrinsic camera calibration and radial lens distortion we applied the widely-used OpenCV calibration tools (opencv.org, 2013). Given that the internal camera parameter does not get changed during the experiments, these were calculated once in our institute. For extrinsic calibration we chose external, easy to mount markers on the fish tank. These can be used to calculate the camera position according to the fish tank's coordinate system. For markers we used red golf balls. With a CNC-milling machine we cut edges in the balls to fit it accurately to the fish tank corners. We fixed six balls on two sides of the fish tank, so that four balls are visible in every camera view (see Figure 2).

2.2.1 Extrinsic Camera Calibration

Extrinsic camera calibration is a well studied problem in computer vision and several tools are available on the market. The most calibration methods estimate the homography between a model plane, which has distinctive known feature points (like a checkerboard), and its image [e.g. (ZHANG, 2000)]. These methods are based on a pinhole camera model and do not take any kind of refraction into account. For that reason these methods cause inaccuracies in applications with cameras outside of a water filled fish tanks. For reducing these inaccuracies it is possible to put the model plane inside the water filled aquarium and calibrate the cameras [e.g. (Butail and Paley, 2012)]. In this case the algorithm balances the refraction by shifting the estimated camera position behind

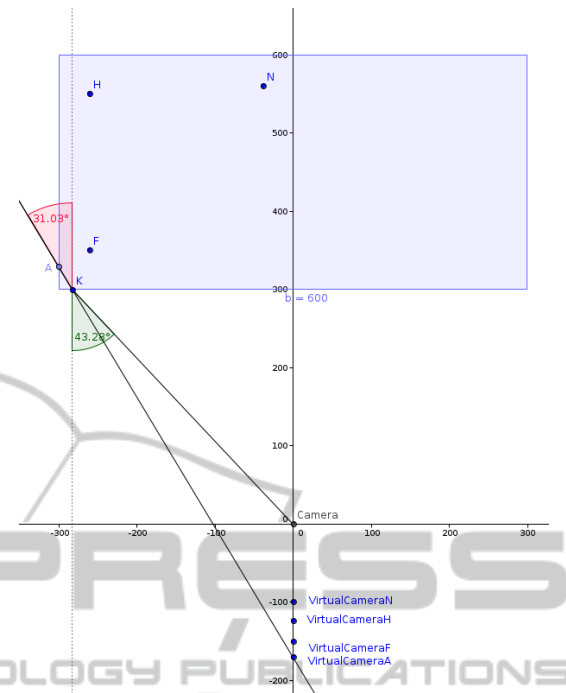


Figure 3: Extrinsic Camera calibration without considering refraction. The estimated camera position $VirtualCamera[H,F,A,N]$ depends on the referred object point inside the water-filled aquarium (A, F, H and N) and is not unique.

the real camera position what compensates the refraction locally. This also reduces the error globally but does not deliver a distinct camera position. As shown in Figure 3 the estimated camera position depends on the location of the referred point.

For that reason we split the calibration in two parts. In the first part we calibrate our cameras referring to the fixed balls outside of the aquarium. In the second part we calculate the refraction of every single camera ray using the refraction law.

Predefinition

For the following calculations we assume that:

- The vector \vec{x} has the components $(x_x, x_y, x_z)^T$.
- A normalized vector is defined as $\hat{x} = \frac{\vec{x}}{|\vec{x}|}$.
- $\vec{x}_{1,2}$ is a short form of \vec{x}_1 and \vec{x}_2 .
- In the following the indices 1 and 2 refer to Camera 1 and Camera 2.

Camera Calibration with Marker Balls

Based on shapes of the balls and their centre positions fixed to the tank corners we assume that the centre

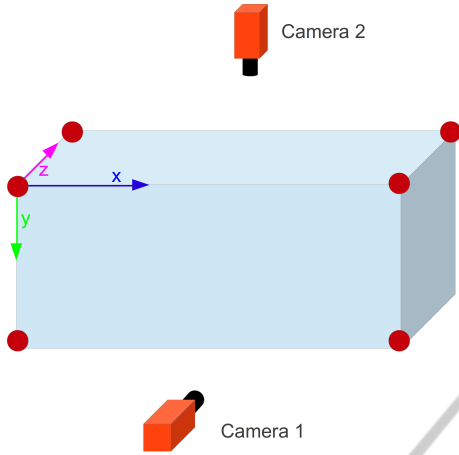


Figure 4: Coordinate system of the fish tank.

of the balls image plain projection also describes the camera ray through the tank corners. We also know the physical dimensions of the fish tank and assume that the xy -plane of our coordinate system lies on the front window with z -axis heading to the back of the tank (see Figure 4). As the balls are painted red we use a colour-based blob detection algorithm for marker identification. By calculating the moment of the segmented balls we get the centre of them. In our tests the standard deviation of the ball centres with 100 samples was below 0.05 pixels.

With the help of four 3D-2D point correspondences obtained from the former step, we calculate positions and poses of the cameras. We solve this problem by using the analytic method presented in (Gao et al., 2003). Gao et al. used an algebraic approach to solve the perspective-three-point problem. The algorithm delivers the camera calibration matrices C_1 and C_2 according to the coordinate system shown in Figure 4. The camera calibration matrices are defined as

$$C_{1,2} = (R_{1,2}|t_{1,2}) \quad (1)$$

with rotation matrix $R_{1,2}$ and translation vector $t_{1,2}$.

Ray Refraction Calculation

In the following calculation we disregard the refraction of the aquarium-glass given that the caused shifting error is less than 0.12 mm in the worst case and is negligible.

For calculating the refraction we trace the ray starting at the projection center of the camera, passing the air-water border through $\vec{i}_{1,2}$ and finally ending up at the object. The starting point (projection center) $\vec{s}_{1,2}$ of the ray is defined as follows:

$$\vec{s}_{1,2} = -R_{1,2}^{-1}\vec{t}_{1,2} \quad (2)$$

We get the ray $\vec{x}_{1,2}$, which starts at the camera project center, by multiplying the inverse of the projection matrix with the according 2D point x' . Given that the projection matrix is singular, we invert it using singular value decomposition.

$$\hat{x}_{1,2} = C_{1,2}^{-1}x' = \frac{\vec{i}_{1,2} - \vec{s}_{1,2}}{|\vec{i}_{1,2} - \vec{s}_{1,2}|} \quad (3)$$

For getting the ray piercing point at the air-water border we compute the length of the ray between \vec{s}_n and \vec{i}_n . Due to the fact that the hit plane for the first camera is identical to the x - y plane and for the second camera parallel to the x - z plane, we simplify the calculation. $c_{1,2}$ describes the length factor:

$$c_1 = \frac{s_{1z}}{s_{1z} - x_{1z}} \quad (4)$$

For the second camera we have to consider the water level w , which is measured manually:

$$c_2 = \frac{s_{2y} - w}{s_{2y} - x_{2y}} \quad (5)$$

Finally we use $c_{1,2}$ to compute the intersection point $\vec{i}_{1,2}$:

$$\vec{i}_{1,2} = c_{1,2}(x_{1,2} - \vec{s}_{1,2}) + \vec{s}_{1,2} \quad (6)$$

The refraction of rays passing from one medium to another is defined by

$$\frac{\sin \alpha}{\sin \beta} = \frac{n_2}{n_1} \quad (7)$$

with the indices of refraction n_1 and n_2 .

For getting α we calculate the angle between the camera ray \vec{x}_1 and the front side of the tank and the camera ray \vec{x}_2 and the water plane. Since these planes are parallel to the coordinate system planes we simplify the calculation.

$$\alpha_1 = \sin^{-1}\left(\frac{x_{1z}}{|\vec{x}_1|}\right) - \frac{\pi}{2} \quad (8)$$

$$\alpha_2 = \sin^{-1}\left(\frac{x_{2y}}{|\vec{x}_2|}\right) - \frac{\pi}{2} \quad (9)$$

Based on (7) we get

$$\beta_n = \sin^{-1}\left(\sin \alpha_{1,2} \frac{n_1}{n_2}\right) \quad (10)$$

The ray is turned in $\vec{i}_{1,2}$ around the axis $\vec{a}_{1,2}$. $\vec{a}_{1,2}$ is perpendicular to the plane between $\vec{x}_{1,2}$ and the center ray of the cameras $\vec{c}'_{1,2}$. c' describes the center pixel of the cameras.

$$\vec{a}_{1,2} = (C_{1,2}^{-1}c') \times \vec{x}_{1,2} \quad (11)$$

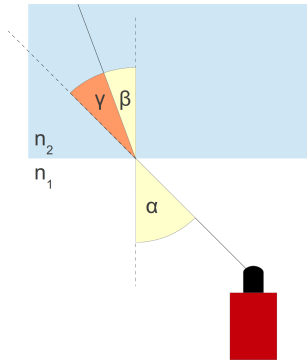


Figure 5: Ray refraction. γ is the angle of refraction.

We calculate a rotation matrix $R_{a_{1,2}}$ with the help of the normalized vector $\hat{a}_{1,2}$. As shown in Figure 5 the final turning angle γ is defined

$$\gamma = \beta - \alpha. \quad (12)$$

$$R_{a_{1,2}} = \begin{pmatrix} d_1 & d_2 & d_3 \\ e_1 & e_2 & e_3 \\ f_1 & f_2 & f_3 \end{pmatrix} \text{ with}$$

$$\begin{aligned} d_1 &= \hat{a}_x^2(1 - \cos \gamma) + \cos \gamma \\ d_2 &= \hat{a}_y \hat{a}_x(1 - \cos \gamma) + \hat{a}_z \sin \gamma \\ d_3 &= \hat{a}_z \hat{a}_x(1 - \cos \gamma) - \hat{a}_y \sin \gamma \\ e_1 &= \hat{a}_x \hat{a}_y(1 - \cos \gamma) - \hat{a}_z \sin \gamma \\ e_2 &= \hat{a}_y^2(1 - \cos \gamma) + \cos \gamma \\ e_3 &= \hat{a}_z \hat{a}_y(1 - \cos \gamma) + \hat{a}_x \sin \gamma \\ f_1 &= \hat{a}_x \hat{a}_z(1 - \cos \gamma) + \hat{a}_y \sin \gamma \\ f_2 &= \hat{a}_y \hat{a}_z(1 - \cos \gamma) - \hat{a}_x \sin \gamma \\ f_3 &= \hat{a}_z^2(1 - \cos \gamma) + \cos \gamma \end{aligned} \quad (13)$$

Finally we get the refracted ray $\vec{x}_{r_{1,2}}$. It starts at $\vec{i}_{1,2}$.

$$\vec{x}_{r_{1,2}} = R_{a_{1,2}} \hat{x}_{1,2} \quad (14)$$

2.3 Segmentation

Fish segmentation is an important part of our work, because the 3D model generation is based on the fish shape information. Therefore, we use a very precise segmentation method which is also robust against fish shadows. Additionally it is simple and fast to initialise. In the future behaviour studies the fish need a period of acclimation in the fish tank. With our approach we can generate the background during the acclimation time automatically.

As the environment of the fish and also the cameras are static the most projects in this scope used background subtraction methods for fish-segmentation (Delcourt et al., 2012). Fontaine et al.

(Fontaine et al., 2008) used a semi-automated routine for an initial detection of fish. They took the first video frame and marked the region around the fish. With the help of a Matlab function they erased the fish and estimated the background model for segmentation.

In our approach we also use background subtraction methods for fish segmentation. We combine two different background subtraction methods and benefit from the advantages of each. On the one hand we use the Gaussian Mixture-based subtraction method (GMS) (Zivkovic, 2004). The GMS method is an adaptive method which adapts the background over time. Especially in scenes with moving foreground objects it is well suited. But if the objects stay at the same place the method starts to add the object to the background. In our project that caused errors especially if fish stay for a longer time at the same place. The detected foreground objects starts to shrink as seen in Figure 6. On the other hand we use a codebook based subtraction method (CB) (Kim et al., 2005). The background of this method is static after initialization and also staying objects get segmented. Normally the background generation of CB is done with background images without foreground objects.

Since we initialize the background during fish swimming inside the tank we split the process into two steps. In the first step we initialize the CB background by using the GMS method. In the second step, the CB method creates a precise foreground.

In the first step the GMS method normally finds at least a small part of the fish like a fin as it is constantly moving and cannot be confused with background. With this information we create a mask around the GMS found foreground objects. Based on center c_n of the contour n , we build a rectangle R_n around c_n with fixed width w and height h values, so that the supposed fish body is covered completely. This mask is applied during computation of the CB background. Background areas which are covered by the mask do not get updated. To ensure that every background pixel is updated sufficiently we count the updates on every pixel. Once every pixel is updated n times, the background generation is finished and the segmentation starts.

Finally we apply a contour-searching algorithm to the CB foreground image and store the contour areas of camera 1 A_{1n} and camera 2 A_{2n} .

2.3.1 Contour Referencing and Mirroring Avoidance

For the 3D ground truth model generation we need pairs of contours (A_{1n}, A_{2n}) from both cameras, which describe the same object. Owing to the fact, that we



Figure 6: Shrunken foreground contour. The fish stayed at the same place for a longer time - as a result the foreground created by GMS shrinks.



Figure 7: Mirrored fish. The fish on the left is mirrored in the right window.

know the path of every camera ray (see section 2.2) we calculate the distance between the camera rays \vec{x}_{r_1} and \vec{x}_{r_2}) of two potential referring contours A_{1n} and A_{2n} .

In order to measure the distance between referring pixel rays (facing the same three dimensional point), we choose the pixel x'_1 and x'_2 with the lowest x-value of the contour. With equation (14) we get the ray of x'_1 and x'_2 and calculate the distance between the two lines. The calculation sequence is described in the following:

```
for (i = 0; i < foundContours_cam1; i++)
{
    pixMinX_Cam1 =
        search pixel with min x of
        foundContours_cam1(i);

    rayCam1 = calculate ray of pixMinX_Cam1;
    for(j = 0; j < foundContours_cam2; j++)
    {
        pixMinX_Cam2 =
            search pixel with min x of
            foundContours_cam2(j);

        rayCam2 = calculate ray of pixMinX_Cam2;

        if(distance(rayCam1, rayCam2) < epsilon)
            store pair(foundContours_cam1(i),
```

```
        foundContours_cam2(j));
    }
}
```

The stored pair of contours describes the same three-dimensional object.

As shown in Figure 7 the fish is mirrored when it comes up to the aquarium glass. In consequence the segmentation system also segments the mirrored fish. With the help of the described technique these mirrored contours get ignored. By matching the contours of both cameras, no suitable contour is found for the mirrored one and it gets deleted.

2.3.2 Shadows

As seen in Figure 8 another problem which occurs during segmentation is shadow segmentation. We solve that problem by adjusting the CB subtraction method. For every pixel the CB background stores one or more ranges of values for every color channel. Only if a tested pixel fits in all of this ranges, it will be accepted as background. Because of this we can expend the luminance channel range of CB, without assessing a pixel as background by mistake. As an effect luminance based changes have only slight influence on the final foreground image.

2.4 3D Ground Truth Model Generation

For our future work, we need a precise 3D model in which we can fit our own created fish model. Particular attention has to be turned to the bending along the roll-axis of the fish, so that we are able to reconstruct the movement of the fish precisely. This is given by the orthogonal camera setup with a camera above the tank. On the other side with this setup, it is not possible to find texture based reference points like in stereo-vision setups. Consequently our method creates a box type fish model that sharply reconstructs the bending along the roll axis and the position.

At first we create a set of triangles along the fish's contour rays $\vec{x}_{r_{1n}}$ from camera 1. n describes the ray number. $\vec{x}_{r_{1n}}$ and $\vec{x}_{r_{1n+1}}$ are neighbouring rays. \vec{i}_{1n} is the starting point of ray $\vec{x}_{r_{1n}}$. Given that we want to create a model inside the fish tank we defined an ending point of ray $\vec{x}_{r_{1n}}$.

$$\vec{e}_n = \hat{x}_{r_{1n}}l + \vec{i}_{1n} \quad (15)$$

l is the maximal ray length inside the tank. The triangles along the contour are defined as follows. For

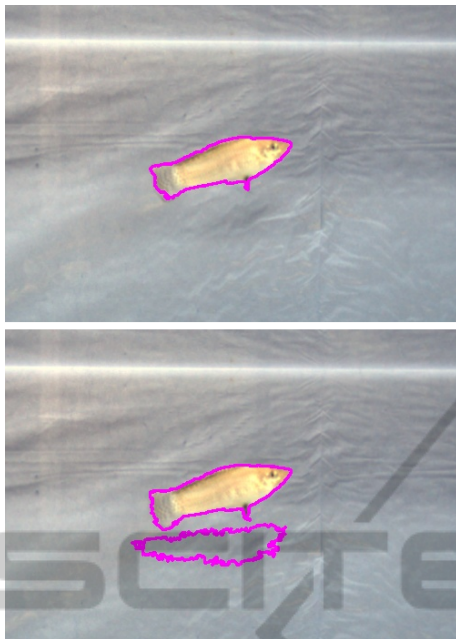


Figure 8: Fish shadow. Segmentation with (upper image) and without (lower image) shadow avoidance.

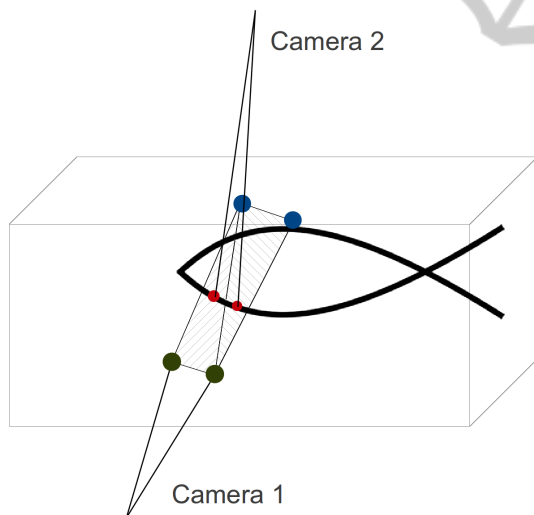


Figure 9: 3D calculation. The contour rays of camera 1 intersect with the front window (green points) pass through the tank and end up at the back window of the tank (blue points). The red points represent the intersection point of contour rays of camera 2 and the spanned triangles of camera 1.

each ray we construct two triangles:

$$\begin{aligned} \Delta_{1n} &= \Delta(\vec{i}_{1n}, \vec{e}_n, \vec{i}_{1n+1}) \\ \Delta_{2n} &= \Delta(\vec{e}_n, \vec{i}_{1n+1}, \vec{e}_{n+1}) \end{aligned} \quad (16)$$

The triangles border the fish contour along the optical axis of camera 1 so that we have a tube in shape of a fish starting at the front side and ending up at the

back side of the tank.

For getting the final 3D ground truth model of the fish we use the fish contour information from the second camera. We calculate the intersection points of the refracted rays \vec{x}_{r2n} (camera 2) and the triangle mesh created in the former step (see Figure 9). The calculation sequence is described in the following pseudo code:

```
for (i = 0; i < n_ray2; i++)
{
  for(j = 0; j < n_ray1; j++)
  {
    if ray2_i intersect triangle1_j
      calculate intersectionPoint;
      store intersectionPoint;
    if ray2_i intersect triangle2_j
      calculate intersectionPoint;
      store intersectionPoint;
  }
}
```

For testing of intersection and calculating the intersection point we use the ray-triangle method of Möller and Trumbore which is explained in (Moeller and Trumbore, 1997).

Finally the detected set of 3D points represents an abstract model of the fish. This model combines besides the absolute position all important moving and bending parameters of the fish.

3 RESULTS

In the following we present the results of calibration, segmentation and 3D ground truth data generation.

3.1 Calibration

In order to test the calibration a reference objects (cuboid of aluminium) was manufactured with a precision of 0.01 mm. We placed it in different locations and orientations in the fish tank and recorded images of it. Afterwards we manually selected the corners of the cuboid in both camera images. Based on the pixel values of the corners we calculated the world coordinates using the extrinsic camera calibration. Finally, we measured the distance between the corners using the method described in Section 2.4. In our tests we got a mean distance (relative) error of 0,31 mm with a standard deviation of 0,22 mm.

For measuring the absolute position error we placed the cuboid in the defined corners of the aquarium and measured the position of the cuboid inner corners as described above. We got a maximal (absolute) error of 2.1 mm. By deactivating the refraction compensation the error increased to 12.6 mm.

3.2 Segmentation

We tested the previously shown segmentation method under various illumination conditions, with fish of different size and with different ground substrates (sand, grit). The initialization of the CB background subtraction with the help of the GMS yielded in reasonable results. Depending on the number of fish the time of initialization varied. In our tests we stopped the initial process after every background pixel was updated at least 50 times. In the worst case the initialisation took up to 60 s. The implemented shadow removal also worked well. During our tests we adjusted the illumination threshold of our background subtraction regarding to the used illumination. We figured out that a high threshold value (very dark shadows) also influences the segmentation negatively. Especially transparent tail fins of female fish were not segmented completely under the described circumstances.

Figure 10 shows some results of the segmentation. As seen in the images the fish was segmented in the images of both cameras. Since the background of the front camera image was more homogeneous than the background of the upper camera, the segmented contour is smoother. The lateral fins of the fish are transparent and were not detected by the algorithm.

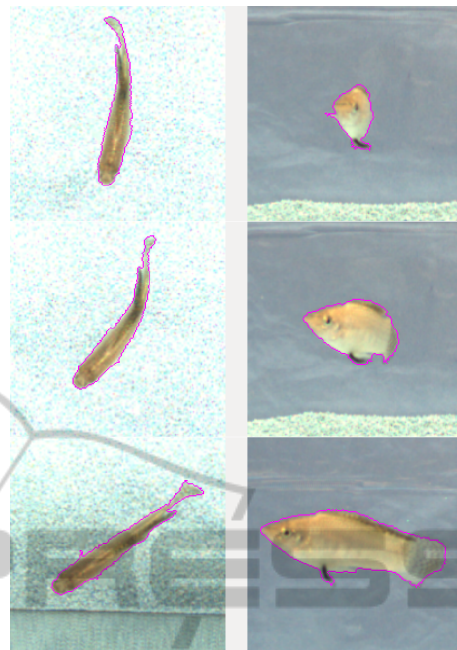


Figure 10: Segmented fish in different pose from the upper camera (left) and the front camera (right).

3.3 3D Ground Truth Model

For visualisation and validation of the 3D ground truth data we developed a 3D viewer, which visualizes the camera rays in real time (see Figure 11). The two camera projection centers are placed in front and above the fish tank. From there the rays are refracted at the air-water border and run through the aquarium. The skew rays of the two cameras approximately intersect inside the aquarium. To get the approximated intersection point, we computed the shortest line between the two skew rays and calculated the center point of the line. This represents the observed 3D object point. As unit of error measurement we defined the distance between the most left rays of first and second cameras' pixel contours. In case of a fish we measured the distance between the pixel rays of the snout. In our test a fish was swimming from one side of the tank to the other side. The measured mean distance between the two rays was 0.64 mm with a standard deviation of 0.72 mm.

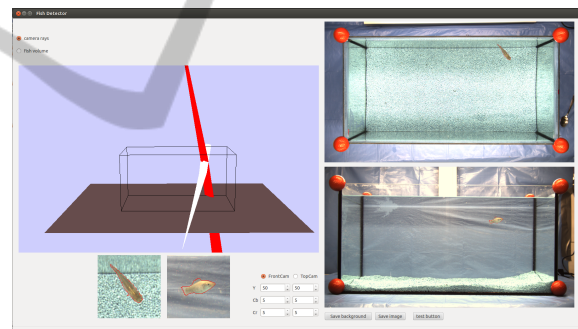


Figure 11: Visualisation tool. On the left it shows the virtual 3D fish tank with the contour rays of the upper camera (red) and the front camera (white). The referring images are shown on the right side.

erating 3D ground truth data of fish in an aquarium considering refraction in real time. With regards to the utilization in fish behavioural studies a well operating and easy to handle application was requested. Taking the water-refraction into account, we achieve a very precise extrinsic camera calibration. As indicated in the results, the relative exactness of the presented method is about ± 0.3 mm. The absolute position error of 2.1 mm is based on the precision of the aquarium manufacturing. It can be decreased by increasing the precision of the aquarium manufacturing.

Furthermore, we established a segmentation method by combining two background subtraction methods – one based on codebook and one adapted

4 CONCLUSIONS

In this paper we presented a novel approach for gen-

from the Gaussian Mixture-based background subtraction method. By doing so, we are able to initialize the background with fish in the tank. In addition, it is possible to exclude mirror images and shadows of the fish easily. The advantages of this approach lie in the high precision combined with an easy utilization in real time. In the future, based on these ground truth data we can adopt fish's behaviour and movements for virtual fish; furthermore the data can serve as a control for the final analysis-by-synthesis system.

ACKNOWLEDGEMENTS

The presented work was developed within the scope of the interdisciplinary, DFG-funded project “virtual fish” of the Institute of Real Time Learning Systems (EZLS) and the Department of Biology and Didactics at the University of Siegen.

REFERENCES

- Bouguet, J.-Y. (2004). Camera calibration toolbox for matlab. <http://www.vision.caltech.edu/bouguetj/calibdoc/> [26.08.2013].
- Butail, S. and Paley, D. A. (2012). Three-dimensional reconstruction of fast-start swimming kinematics of densely schooling fish. *Journal of The Royal Society Interface*, 9:77–88.
- Delcourt, J., Denoel, M., Ylieff, M., and Poncin, P. (2012). Video multitasking of fish behaviour: a synthesis and future perspectives. *Fish and Fisheries*, 14:186–204.
- Fontaine, E., Lentink, D., Kranenbarg, S., Mueller, U. K., van Leeuwen, J. L., Barr, A. H., and Burdick, J. W. (2008). Automated visual tracking for studying the ontogeny of zebrafish swimming. *Journal of Experimental Biology*, 211:1305–1316.
- Gao, X. S., Hou, X. R., Tang, J., and Cheng, H. F. (2003). Complete solution classification for the perspective-three-point problem. *IEEE Transactions on Pattern Analysis and Machine Intelligence*, 25(8):930–943.
- Kim, K., Chalidabhongse, T. H., Harwood, D., and Davis, L. (2005). Real-time foreground-background segmentation using codebook model. *Real-time imaging*, 11(3):172–185.
- Kuhnert, L., Thamke, S., Ax, M., Nguyen, D., and Kuhnert, K.-D. (2012). Cooperation in heterogeneous groups of autonomous robots. *International Conference on Mechatronics and Automation (ICMA) IEEE*, pages 1710–1715.
- Laurel, B. J., Laurel, C. J., Brown, J. A., and Gregory, R. S. (2005). A new technique to gather 3d spatial information using a single camera. *Journal of Fish Biology*, 66:429–441.
- Moeller, T. and Trumbore, B. (1997). Fast, minimum storage ray-triangle intersection. *Journal of graphics tools*, 2.1:21–28.
- opencv.org (2013). Opencv — opencv. <http://opencv.org/> [01.09.2013].
- Quigley, M., Conley, K., Gerkey, B., Faust, J., Foote, T., Leibs, J., Wheeler, R., and Ng, A. Y. (2009). Ros: an open-source robot operating system. In *ICRA workshop on open source software*, volume 3.
- Yamashita, A., Kawanishi, R., Koketsu, T., Kaneko, T., and Asama, H. (2011). Underwater sensing with omnidirectional stereo camera. In *Computer Vision Workshops (ICCV Workshops), 2011 IEEE International Conference*.
- ZHANG, Z. (2000). A flexible new technique for camera calibration. *IEEE Transactions on Pattern Analysis and Machine Intelligence*, 22.11:1330–1334.
- Zhu, L. and Weng, W. (2007). Catadioptric stereo-vision system for the real-time monitoring of 3d behaviour in aquatic animals. *Physiology & Behavior*, 91:106–119.
- Zivkovic, Z. (2004). Improved adaptive gaussian mixture model for background subtraction. In *Pattern Recognition, 2004. ICPR 2004. Proceedings of the 17th International Conference on*, volume 2, pages 28–31. IEEE.